ACS APPLIED MATERIALS & INTERFACES
Forum Article
www.acsami.org

Tunable Hydrophilic or Amphiphilic Coatings: A “Reactive Layer Stack” Approach

Ralf Frenzel, Susanne Höhne,* Christian Hanzelmann, Thomas Schmidt, René Winkler, Astrid Drechsler, Eva Bittrich, Klaus-Jochen Eichhorn, and Petra Uhlmann*

Leibniz-Institut für Polymerforschung Dresden e.V., Hohe Strasse 6, D-01069 Dresden, Germany

Supporting Information

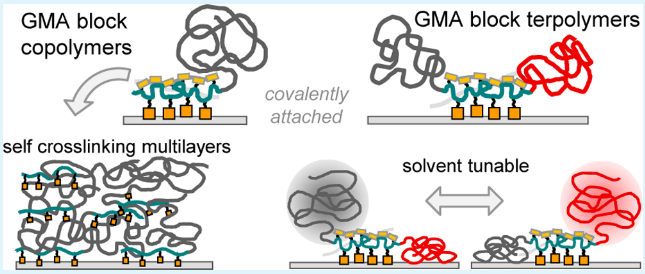

ABSTRACT: Thin films with tunable properties are very interesting for potential applications as functional coatings with, for example, anti-icing or improved easy-to-clean properties. A novel “reactive layer stack” approach was developed to create covalently grafted mono- and multilayers of poly(glycidyl methacrylate)/poly(*tert*-butyl acrylate) diblock copolymers. Because these copolymers contain poly(glycidyl methacrylate) blocks they behave as self-cross-linking materials after creation of acrylic acid functionalities by splitting off the *tert*-butyl units. The ellipsometrically determined coating thickness of the resulting hydrophilic multilayers depended linearly on the number of applied layers. Amphiphilic films with tunable wettability were prepared using triblock terpolymers with an additional poly(methyl methacrylate) block. The mechanism of the formation of the (multi)layers was investigated in detail by studying the acidolysis of the surface-linked *tert*-butyl acrylate blocks by infrared reflection absorbance spectroscopy, accompanied by surface analysis using atomic force microscopy and contact angle measurements. In the case of the amphiphilic and switchable terpolymer layers this reaction was very sensitive to the used acidic reagent.

KEYWORDS: *glycidyl methacrylate, IRRAS, triblock terpolymers, anchor block, multilayers, self-cross-linking polymer layers*

INTRODUCTION

Transparent coating of metals and other substrates with functional polymer layers is of technical interest to provide surface finishes with special properties like adjustable hydrophobicity or protection against weathering, pollution, fouling, or icing. Often it is desired that the optical performance of the coated substrate is not changed by the applied coating. This and the reduction of costs require the application of very thin films. One versatile possibility to control surface properties purposefully and sustainably is to link polymers or block copolymers stably and permanently to surfaces. For a covalent linking mainly the “grafting from” and “grafting to” strategies are used.[1−4] Grafting from methods (Figure 1A) involve the covalent attachment of an initiating group followed by chain polymerization of suitable monomers.[5,6] Separately synthesized end-functionalized polymers can be attached to the surface by various grafting to methods (Figure 1B). Common approaches include the reaction of a terminally functionalized polymer that has native functional groups of the substrate surface with reactive groups of a monolayer or with functional groups of a primary polymer layer.[7,8] For the primary polymer layer approach a thin polymer (mono-) layer is applied, which serves both as initial surface layer and as reactive anchoring layer. For this purpose the primary polymer must have functional groups reactive to the native surface groups and to the end groups of the polymers to be tethered. Using the grafting to approach also block copolymers with reactive groups in an inner block or copolymers with reactive side chains can be attached to a surface.[9,10] In the case of a block terpolymer the former method results in a layer with highly mobile outer blocks as shown in Figure 1C. The combination of block copolymers having a reactive component with this primary polymer layer approach results in an additionally cross-linked and therefore very stable surface layer as sketched in Figure 1D.

Alternatively a physical attachment of the polymers can be sufficient if the polymer layers are cross-linked and therewith insoluble.

Covalently interconnected polymer multilayers can be obtained by cross-linking of functional polymers or using reactive di- or multifunctional small molecules.[11−15] Recently a copolymer-based multilayer approach was presented generating surface-attached polymer networks through thermal cross-linking of polymers containing sulfonyl azide groups.[16]

Poly(glycidyl methacrylate) (PGMA), here used as the species responsible for cross-linking and anchoring, is a versatile, reactive polymer since the pendant oxirane ring can be opened for cross-linking or other reactions introducing a

Special Issue: Forum on Polymeric Nanostructures: Recent Advances toward Applications

Received: October 24, 2014
Accepted: December 17, 2014
Published: January 8, 2015

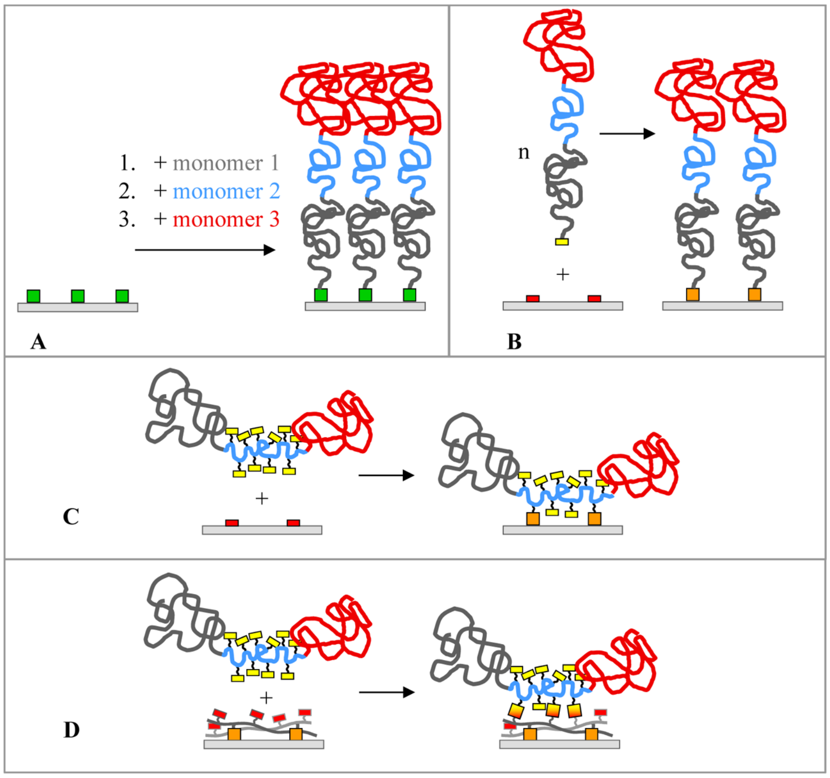

Figure 1. Strategies for grafting of triblock terpolymers on surfaces: (A) grafting from technique using sequential monomer addition on an initiator-functionalized surface, (B) grafting to technique with an end-group functionalized triblock terpolymer, (C) attachment of a triblock terpolymer with an inner anchor block, and (D) attachment of the triblock terpolymer on a primary polymer layer.

wide range of functionalities. The glycidyl group is able to self-cross-link or to be linked to functional groups such as amino, hydroxyl, or carboxyl groups on the surface of a substrate. Because of its reactivity and versatility PGMA is frequently used as a primary coating for the attachment of different polymer brushes.[8,17,18]

Tert-butyl groups (*t*Bu) in acrylates or methacrylates are convenient precursors in the synthesis and layer formation of carboxylate-containing polymers. Generally *t*Bu esters are used as protecting groups for carboxyl moieties, for instance, in peptide chemistry.[19] Recently, the reaction became important for microelectronic processing by using it for the conversion of polymer films during photolithographic processes.[20,21] The splitting off reaction yielding the free carboxylic acid can be realized by different methods and reagents. In all cases the reaction is started by a protonation step followed by elimination of isobutene (see Figure 3b). In contrast to ester hydrolysis no water is involved in the reaction course. This reaction permits the selective release of carboxyl groups from *t*Bu esters also in the presence of other ester moieties because of its faster cleavage in comparison to methyl or other alkyl esters and irreversible elimination of isobutene. Hence, the reaction is catalyzed by strong Brønsted acids. For the prevention of side reactions like substitution and hydrolysis the use of acids with less polarizable anions (like sulfonic or perfluorocarboxylic acids) and aprotic solvents is advantageous.

Well-established is the cleavage of *t*Bu esters using hydrochloric acid in dioxane yielding quantitatively the carboxylic acids in solution and on surfaces.[22,23] The use of *p*-toluenesulfonic acid in benzene is a well-known method for the acidolysis of *t*Bu esters in brushes.[24] Recently, methanesulfonic acid was used for this reaction to produce micropatterned polymer layers, too.[25] On surfaces the carboxylic acid groups can be used as reactive functionalities or for the generation of hydrophilic and amphiphilic layers.

The monitoring of the complete splitting off of the *t*Bu groups is often an analytical problem especially in the case of very thin layers. In principle IR spectroscopic investigations are suitable to investigate chemical changes in polymer layers. For measurements in transmission mode the substrate must be IR-transparent, and the polymer layers should have an adequate thickness to reach sufficient signal intensity. This technique is inapplicable in the case of metal substrates because of their optical impermeability. In contrast, reflection spectra of very thin layers can be obtained using the infrared reflection absorbance spectroscopy (IRRA spectroscopy or IRRAS) technique. This method uses p-polarized light and a grazing angle of incidence (∼80°). Under ideal conditions even spectra of monolayers of organic molecules can be recorded.[26]

Amphiphilic block co- and terpolymers are expected to self-organize at surfaces if definitive differences in polarity of their segments are present.[27] Mixed hydrophilic/hydrophobic domains of antifreeze (glyco) proteins (AF(G)P)s in organisms of the polar and subpolar regions are presumed to make a significant contribution to the inhibition of intracellular ice crystal growth. Some attempts to attach antifreeze proteins onto surfaces show that it is possible to transfer the activity of these molecules from solution to surfaces.[28,29] Because of the limited availability and high costs of AF(G)Ps it is of interest to mimic these biological structural features by artificial macromolecules. Therefore, it was a goal of this study to investigate the structure formation of amphiphilic block co- and terpolymers on surfaces. Furthermore, it is known that hydrophilic surface-attached polymers may reduce the freezing point on surfaces due to their colligative effect.[30,31] It was therefore reasonable to generate also hydrophilic polymer layers that were supposed to serve as freezing point reducing coatings.

For this purpose diblock copolymers containing a poly(*tert*-butyl acrylate) P*t*BA and a shorter PGMA anchor block (which in most cases contains also P*t*BA units)[32] were used to produce smooth hydrophilic polymer layers on aluminum and silicon wafer surfaces. Aluminum was selected as a typical technically used metal substrate. Mono- and multilayers of the copolymers were prepared to obtain sustainable layers with defined thicknesses. In a similar way, amphiphilic surface coatings were created using triblock terpolymers consisting of a P*t*BA, a P(*t*BA-*b*-GMA), and a PMMA block. The IRRAS technique was applied for the chemical characterization of polymer films up to 15 nm thickness on aluminum surfaces and for the examination of the splitting off of the *t*Bu groups present in the P*t*BA blocks of these films. Comprehensive thin-film analysis was done using atomic force microscopy (AFM) and contact angle measurements.

■ EXPERIMENTAL SECTION

Materials. *Tert*-butyl acrylate (*t*BA), glycidyl methacrylate (GMA), and methyl methacrylate (MMA) were distilled and stored at −20 °C under argon prior to use. CuBr (98%), $CuBr_2$ (99%), and CuCl (99.995+ %) (Sigma-Aldrich) were purified with glacial acetic acid and washed with pure ethanol and diethyl ether, then stored under argon. *N*,*N*,*N*′,*N*′,*N*″-Pentamethyldiethylenetriamine (PMDETA, 99%), 1,1,4,7,10,10-hexamethyltriethylene tetramine (HMTETA, 97%), methyl 2-bromopropionate (MBrP, 98%), *p*-toluenesulfonic acid monohydrate (98,5%), methanesulfonic acid (≥99.5%), and trimethyl benzylsilane (99%) were obtained from Sigma-Aldrich and used as received.

Poly(glycidyl methacrylate) (PGMA), M_n = 17 500 g/mol, M_w/M_n = 1.7, and carboxyl-terminated poly(*tert*-butyl acrylate) (P*t*BA-COOH), M_n = 42 000 g/mol, M_w/M_n = 1.1, were purchased from Polymer Source, Inc. (Canada).

All other reagents and solvents were commercial products and used as received unless otherwise stated. Highly polished single-crystal silicon wafers (Si wafers) of {100} orientation (Si-Mat Silicon Materials, Germany) and 200 nm thick vapor-deposited aluminum layers at Si wafers (Silicon Materials, Landsberg am Lech) were used as a substrate for the polymer layer preparation.

Synthesis of P*t*BA-Br. Copper bromide, ligand, solvent, and *t*BA (B1:0.0392 g of CuBr, 0.0473 g of PMDETA, 2 mL of anisole, and 7.0000 g of *t*BA) were placed in a Schlenk flask, which was then filled with argon, and the mixture was degassed three times by freeze−pump−thaw cycles. The ratio of copper halide to ligand was always one. For the determination of conversion and molecular weight a sample (reference) was taken at this time. The initiator was added (B1:0.0456 g), and the mixture was heated to reaction temperature (60 °C). During the course of reaction samples were taken from the reaction mixture, dissolved in $CDCl_3$, cooled, and analyzed by ^1H NMR spectroscopy (the residual concentration of monomer was determined with trimethyl benzylsilane or anisole as an internal standard). Prior to size exclusion chromatography (SEC) analysis, these samples were passed through a small neutral alumina column to remove catalyst, concentrated, and precipitated. Upon completion of the polymerization, the reaction mixture was cooled, dissolved in acetone, and passed through a neutral alumina column to remove the catalyst. Then the polymer solution was concentrated using a rotary evaporator, taken up with a low quantity of diethyl ether, and precipitated in a methanol/water mixture (1:1). For purification the polymer was dissolved in diethyl ether and reprecipitated in a methanol/water mixture (1:1) twice.

Synthesis of P(*t*BA-*b*-[*t*BA-*co*-GMA]). The *t*BA polymerization was started as described above. The desired amount of GMA together with copper chloride and HMTETA was purged with argon, and after achieving 70−90% conversion of *t*BA this mixture was added to the reaction mixture. Further polymerization was carried out at 50 °C. The purification was carried out as described for P*t*BA-Br but as solvent DCM was used, and the polymer was precipitated in pentane.

Synthesis of P(*t*BA-*b*-GMA). The P*t*BA-Br was placed together with GMA and the solvent in a Schlenk flask. After dissolution of the macroinitiator the mixture was degassed three times by freeze−pump−thaw cycles. The copper chloride and the ligand were added before the last cycle. The polymerization and purification were carried out as described for the P(*t*BA-*b*-[*t*BA-*co*-GMA]).

Synthesis of P(*t*BA-*b*-[*t*BA-*co*-GMA])-*b*-MMA). The P(*t*BA-*b*-[*t*BA-*co*-GMA]) macroinitiator was placed together with MMA and the solvent in a Schlenk flask (T10:2.8100 g of macroinitiator, 1.0638 g of MMA, 0.0070 g of CuCl, 0.0163 g of HMTETA, 5.6 mL of anisole). After dissolution of the macroinitiator the mixture was degassed three times by freeze−pump−thaw cycles. The copper halide and the ligand were added before the last cycle. The polymerization was carried out at 50 °C. Upon completion of the polymerization the reaction mixture was cooled, dissolved in tetrahydrofuran (THF), and passed through a neutral alumina column to remove the catalyst. Then the polymer solution was concentrated using a rotary evaporator and precipitated in pentane. For purification the polymer was dissolved and reprecipitated twice in pentane.

Polymer Film Preparation. The bare and aluminum-sputtered Si wafers were cleaned with absolute ethanol for 20 min in an ultrasonic bath. To remove residual organic contaminants and to activate their surfaces the wafers were subsequently exposed to oxygen plasma (Plasma G440 of Technics Plasma Inc. Kirchheim, Germany) at 100 W for 60 s.

The PGMA anchor layer was prepared by spin-coating 80 μL of a 0.02 wt % solution of PGMA in $CHCl_3$ at a velocity of 2000 rpm with an acceleration of 1000 rpm/s for 10 s and annealing it for 20 min at 100 °C in a vacuum oven.

The P*t*BA model layers, the block copolymer, and the triblock terpolymer layers were prepared by spin-coating 100 μL of a 1 wt % solution of the polymer in THF on the wafer 0.5 h after the plasma treatment (velocity 2500 rpm, acceleration 1000 rpm/s, time 10 s). This solution was filtered with a Teflon filter having pore sizes of 0.2 μm before the spin-coating process. The freshly prepared film was dried and annealed at 100 °C for 16 h under slight vacuum. Afterward, all unbonded polymer was removed by solvent extraction in a Soxhlet apparatus. The samples were dried in a stream of nitrogen.

Elimination of the *t*Bu Moieties in the Layers. (A)[24] The wafers were put into a solution of benzene saturated with *p*-toluenesulfonic acid monohydrate (Aldrich) during 50 min at 55 °C. Afterward the wafers were extensively rinsed (three times 5 min under thorough stirring) with absolute ethanol and dried.

(B)[25] At room temperature the wafers were put into a solution of 2 mL of methanesulfonic acid in 60 mL of dichloromethane (DCM) for 50 min under stirring. Afterward the wafers were extensively rinsed with absolute ethanol as described above and dried.

After each step the layer thickness was determined by ellipsometry.

For the preparation of multilayers the spin-coating process, the annealing, and the splitting off of the *t*Bu groups were repeated in this order up to ten times.

Methods. To determine molecular (M_w) weights and polydispersity indices of the polymers SEC measurements were performed on a PL-GPC 50 Plus from Polymer Laboratories with a PL-AS RT auto sampler, a micro volume double piston pump (10 μL per stoke), and a PC-RI refractive index detector using a light-emitting diode with a wavelength of 880 nm. The eluent THF was injected with a flow rate of 1 mL/min at 40 °C on a 2 × PLgel 5 μm MIXED-D column (600 × 7.5 mm). The linear M_w operating range for this column is 200 to 400 000 g/mol (PS equiv). We used the polystyrene (PS) standards Easi cal PP-2 Standards from Polymer Laboratories, which contained PS with M_w from 580 g/mol (the lowest) to 377 400 g/mol (the highest). Molecular masses were calculated versus these PS standards.

^1H NMR spectra were recorded on a Bruker Avance 250 with $CDCl_3$ as solvent at room temperature. The molecular weights of diblock copolymers were determined by analysis of their ^{1}H NMR spectra using the intensity ratios of the initiator headgroup, the CH acrylate group, and the signals of the epoxy-CH_2 group, respectively. For the calculation of the block length and molecular weights of the triblock terpolymers we utilized the ratio of the PGMA/PMMA groups and calculated the real length of the third block with the help of the results of the corresponding diblock copolymers.

Ellipsometry was performed to evaluate layer thicknesses at $\lambda = 633$ nm and an angle of incidence of 70° using an ellipsometer SE 402 (SENTECH Instruments GmbH, Berlin, Germany). The measurements were performed after each modification step to use the results of the previous measurement as reference for the simulation of ellipsometric data. First, the thickness of the native SiO_2 layer was calculated using a refractive index of $n = 1.4598$. The optical constants of Si were taken from the literature.[33] Then the thickness of the polymer layer was evaluated using a two-layer model SiO_2/polymer. In case of a second grafted layer (model layers) this was done with the three-layer model SiO_2/PGMA/P*t*BA-COOH with fixed refractive indices (1.525 for PGMA and 1.466 for P*t*BA). For the PGMA/P*t*BA block copolymers and PGMA/P*t*BA/PMMA block terpolymers $n = 1.50$ was assumed. In the case of the aluminum-coated Si wafers the effective optical constants of the opaque aluminum layer (as bulk aluminum substrate) were determined for every sample and used instead of silicon/silicon dioxide in the optical model. For the determination of the thicknesses of the swollen multilayers a spectroscopic ellipsometer (M-2000, Woollam Co., Inc., Lincoln NE, U.S.A.) equipped with a rotating compensator was used to measure the ellipsometric data of the polymer layers in the dry state as well as in situ in purified H_2O within a batch cuvette (TSL Spectrosil, Hellma, Muellheim, Germany). These measurements were performed in the visible spectral range between 370 and 900 nm at an angle of incidence Φ_0 of 70°, which is close to the Brewster angle of silicon. To evaluate the refractive index and thickness of the polymer films in dry state and in situ, a multilayer-box-model consisting of silicon, silicon dioxide, and the polymer layer was applied.[34] All data were acquired and analyzed using the CompleteEASE software package (version 4.46).

To characterize the polymer layers, several parameters were calculated. The surface coverage (adsorbed amount), Γ (mg/m^2), was calculated from the ellipsometry thickness of the layer, d (nm), by the following equation:

$$\Gamma = d\cdot\rho$$

where ρ is the density of the attached macromolecules.

The grafting density, σ (chains/nm^2), that is, the inverse of the average area per adsorbed chain, was determined by

$$\sigma = N_A\cdot\Gamma/M_n$$

where N_A is Avogadro's number and M_n (g/mol) is the number-average molar mass of the grafted polymer.[18] Supporting Information, Table ST1 summarizes these results.

The AFM measurements were done in the soft tapping mode using a Dimension 3100 NanoScope IIIa (Veeco Instruments, Inc., U.S.A.). We used silicon cantilevers (BudgetSensors, Bulgaria) with a spring constant of ca. 3 N/m and a resonance frequency of ca. 75 kHz; the tip radius was lower than 10 nm. During the scan, a surface morphology image and a phase image were recorded simultaneously. The scan conditions (free amplitude >100 nm, set point amplitude ratio 0.5) were adjusted according to Magonov[35] to get a stiffness contrast in the phase image.

In the dynamic contact angle measurements, advancing (θ_a) and receding (θ_r) contact angles were determined in sessile drop experiments employing the OCA 40 micro (Software SCA 202; Dataphysics GmbH, Filterstadt, Germany). As test liquid freshly deionized water was used. For the contact angle values (θ_a and θ_r) given here, more than seven single measurements on different places on the sample surface were averaged (the standard deviation was smaller than 2°).

IRRA spectra were taken using an Equinox 55 Fourier transform infrared spectrometer (FTIR, Bruker) with a KRS5 polarizer. The carefully purged spectrometer was equipped with a grazing incidence reflection unit and an MCT detector (cooled with liquid nitrogen). All spectra were taken with 4 cm^{-1} resolution with 3000 scans per each measurement at an angle of incidence of 80° relative to the surface normal. The spectra were further processed by carrying out atmospherical compensation (residual water vapor and carbon dioxide) and a baseline correction.

ATR-FTIR spectroscopic measurements were performed to obtain spectra of the pure substances using a Vertex 80v FTIR spectrometer (Bruker) with a "Golden Gate" ATR unit (SPECAC). The spectra were recorded with a resolution of 4 cm^{-1}, and 100 scans were added. An MCT detector was applied. IR transmission measurements of layers on silicon wafers were also done in vacuum with a Vertex 80v and an MCT detector. The spectra were again recorded with a resolution of 4 cm^{-1}, but 3000 scans were added. The spectrum of a pure wafer was used as background spectrum and applied for the baseline correction.

Comparison of an IRRA spectrum of the triblock terpolymer T1 as thin layer (ca. 15 nm thick) on Al and a spectrum of T1 in bulk state (Figure S1 in the Supporting Information) proves that the quality of the IRRA spectra of the polymer films on aluminum is satisfactory and that the characteristic bands of the polymers are visible.

RESULTS AND DISCUSSION

Diblock copolymers and triblock terpolymers containing PGMA blocks were used to produce smooth polymer layers on native and aluminum-coated Si wafers. Both materials have thin native surface oxide layers (2–5 nm thick) passivating them against further corrosion, which can be used for the grafting of polymer coatings. The polymer layers were prepared by spin-coating and subsequent annealing.

Block co- and block terpolymers were synthesized by ATRP as described in our previous paper.[32] They contain blocks of different lengths as listed in Table 1.

Table 1. Polymers for the Layer Preparation

no.	polymer structure (NMR)	M_n (g·mol^{-1}), NMR	M_n (g·mol^{-1}), SEC	PDI
B1	P(*t*BA$_{183}$-*b*-GMA$_5$)	24 269	24 537	1.14
B2	P(*t*BA$_{250}$-*b*-[*t*BA$_{57}$-*co*-GMA$_6$])	40 373	39 087	1.14
B3	P(*t*BA$_{306}$-*b*-[*t*BA$_{13}$-*co*-GMA$_{16}$])	43 418	46 485	1.10
T1	P(*t*BA$_{194}$-*b*-[*t*BA$_{59}$-*co*-GMA$_{36}$]-*b*-MMA$_{80}$)	45 721	24 046	1.31
T2	P(*t*BA$_{94}$-*b*-[*t*BA$_{13}$-*co*-GMA$_{22}$]-*b*-MMA$_{130}$)	29 995	31 887	1.26

As result of the synthetic approach, the PGMA block contained in most cases additional units of P*t*BA in various parts.[32] Figure 2 shows the structures of the used polymers.

Table 2 gives an overview of the model polymer, P*t*BA/PGMA diblock copolymer, and P*t*BA/PGMA/PMMA triblock terpolymer layers, their thicknesses determined by ellipsometric measurements and contact angles. The multilayers were obtained following the "reactive layer stack" approach as described in the text below.

From the layer thicknesses the surface coverage Γ and grafting density σ were calculated. This was done using density and molecular weight of the mobile P*t*BA block in case of the block copolymers B1–B3. For the triblock terpolymers a calculation was done only for the layers after acidolysis. Before acidolysis a mixture of polymers is present in the layers with unknown density. After aqueous treatment the density and molecular weight of the PAA block, and in case of toluene treatment the data of the PMMA block were used for the

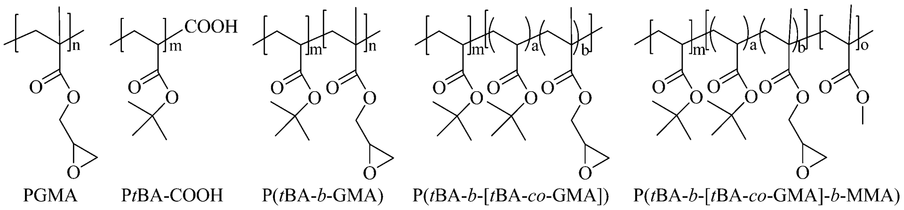

Figure 2. Structures of the used polymers.

Table 2. Polymer Layers on Silicon (Si) and Aluminum-Coated Silicon Wafers (Al) and Characteristic Parameters of the Layers[a]

layer	d^b (nm)	θ_a^{c} (deg)	θ_r^{c} (deg)	layer	d^b (nm)	θ_a^{c} (deg)	θ_r^{c} (deg)
Si/PGMA	2.3 ± 0.1	68 ± 2.0	72 ± 2.0	Al/PGMA	2.0 ± 0.1		
Si/PGMA/P*t*BA	10.5 ± 0.5	88 ± 2.0	65 ± 2.0	Al/PGMA/P*t*BA	10.2 ± 0.1	89 ± 2.0	64 ± 2.0
Si/PGMA/PAA	5.4 ± 0.1	30 ± 3.2	n. d.	Al/PGMA/PAA	5.4 ± 0.1	36 ± 4.5	n. d.
Si/B1	9.7 ± 0.1			Al/B1	9.1 ± 0.2		
Si/B1−H*[c]	5.5 ± 0.1			Al/B1−H*	3.6 ± 0.2		
Si/B1−H*−H_2O	7.3 ± 0.6						
Si/B1 ten layers	57.7 ± 1.0						
Si/B1−H* ten layers	50.7 ± 0.5						
Si/B2	9.5 ± 0.1	89 ± 2.0	73 ± 2.0	Al/B2	8.7 ± 0.3		
Si/B2−H*	5.3 ± 0.3	38 ± 11.0	n. d.	Al/B2−H*	4.1 ± 0.1		
Si/B2−H*−H_2O	7.7 ± 0.1						
Si/B2 ten layers	55.6 ± 0.5						
Si/B2−H* ten layers	48.0 ± 0.5						
Si/B3	11.2 ± 0.1			Al/B3	10.3 ± 0.1		
Si/B3−H*	6.6 ± 0.4			Al/B3−H*	5.3 ± 0.2		
Si/B3−H*−H_2O	9.1 ± 0.5						
Si/B3 ten layers	69.1 ± 0.8						
Si/B3−H* ten layers	60.8 ± 0.9						
Si/T1	12.9 ± 0.3	89 ± 2.0	71 ± 2.0	Al/T1	14.8 ± 1.2		
Si/T1−H*	9.6 ± 0.3			Al/T1−H*	11.5 ± 1.1		
Si/T1−H*−H_2O	10.3 ± 0.7	62 ± 8.4	n. d.				
Si/T1−H*−toluene	9.5 ± 0.4	91 ± 2.3	n. d.				
Si/T1−H**[c]	9.0 ± 0.3			Al/T1−H**	9.0 ± 0.6		
Si/T1−H**−H_2O	9.0 ± 0.3	31 ± 2.0	n. d.				
Si/T1−H**−toluene	9.2 ± 0.3	91 ± 3.3	n. d.				
Si/T2	5.2 ± 0.1	89 ± 2.0	68 ± 2.0	Al/T2	4.5 ± 0.1		
Si/T2−H**	4.1 ± 0.1			Al/T2−H**	3.2 ± 0.1		
Si/T2−H**−H_2O	4.9 ± 0.1	35 ± 2.0	n. d.				
Si/T2−H**−toluene	4.7 ± 0.1	84 ± 2.8	n. d.				

[a] All layers were annealed for 16 h at 100 °C and extracted with THF. H denotes conversion of the P*t*BA blocks to poly(acrylic acid) (PAA) and rinsing with ethanol. H_2O denotes hydrophilic switching by treatment with water. Toluene denotes hydrophobic switching by treatment with toluene. Polymer numbers are according to Table 1. n. d. indicates not detectable. [b] Ellipsometric determinated layer thicknesses *d*. [c] Wetting behavior by water: θ_a advancing contact angle, θ_r receding contact angle. *Splitting off of the *t*Bu unit was done with *p*-toluenesulfonic acid. **Splitting off of the *t*Bu unit was done with methanesulfonic acid.

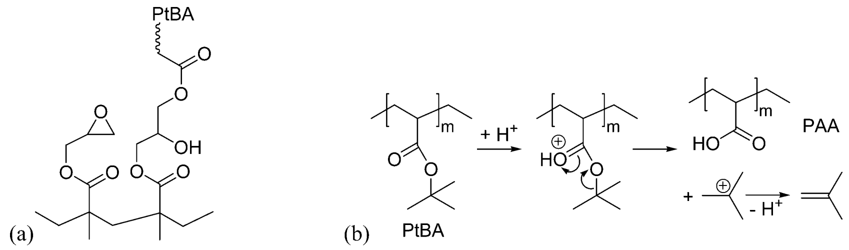

Figure 3. (a) Structure of the grafted P*t*BA brushes and (b) transformation reaction of P*t*BA to PAA.

calculation. The data are discussed in the corresponding sections.

Model Homopolymer Brushes. For the conversion of *t*BA into acrylic acid units in polymers different methods are known.[22−25] To test if the selected method with *p*-toluenesulfonic acid[24] as catalyst is appropriate for the intended layers of block co- and terpolymers (as listed in Table 1) on silicon and aluminum-coated silicon wafers, model layers of *t*BA homopolymers were produced using a primary polymer layer approach.[18] Furthermore, these model brushes were used to test the suitability of the IRRAS method to verify the splitting off of the *t*Bu groups in P*t*BA blocks. As primary polymer layer PGMA homopolymer was used. The P*t*BA brushes were produced by grafting carboxyl-terminated P*t*BA blocks (P*t*BA-COOH) onto the PGMA layer.[24] The polymer layers on silicon and aluminum are similar in thickness and wetting behavior. Detected differences of the PGMA layer thicknesses are not significant due to the low absolute thicknesses of these films. Figure 3a shows schematically the resulting structure. After release of the carboxyl groups by elimination of isobutene, the layers consist of poly(acrylic acid) brushes (Figure 3b).

Figure 4 shows the IRRA spectrum of the Al/PGMA layer in comparison with the IRRA spectra of Al/PGMA/P*t*BA and Al/PGMA/PAA films. The quality of the IRRA spectra of the polymer films on aluminum is satisfactory, and the characteristic bands of the polymers are visible.

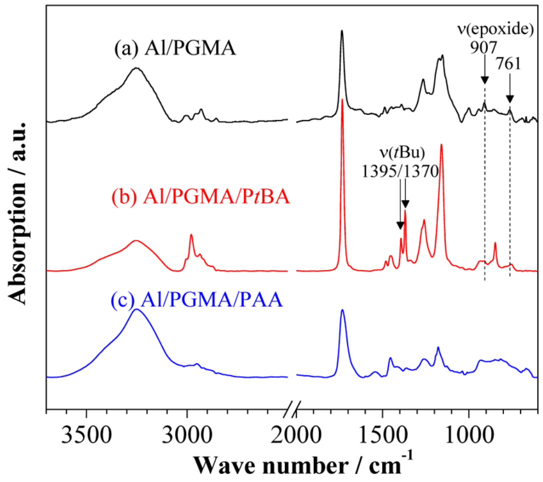

Figure 4. IRRA spectra of (a) Al/PGMA, (b) Al/PGMA/P*t*BA, and (c) Al/PGMA/PAA obtained from (b) catalyzed with *p*-toluenesulfonic acid.

Usually, for the detection of the conversion of P*t*BA to PAA by IR spectroscopy the change of the carbonyl stretching vibration absorption ν(C═O) at ∼1700 cm^{-1} is used.[20] Mostly the carbonyl absorption has the highest intensity in the spectra. But this absorption band is not sufficiently specific in the case of mixed polymer structures containing other carboxylic ester groups. Therefore, we used a characteristic deformation band (symmetric bending vibration) of the tertiary butyl group,[36] namely, the double band at ν(*t*Bu) = 1370 and 1395 cm^{-1}, to verify the progress of the cleavage reaction.

Figure 4b shows the double band assigned to the *t*Bu group in the spectral range of 1360−1400 cm^{-1}. The spectrum shows furthermore the typical acrylate ester bands at 1734 cm^{-1} (C═O stretching vibration), the methyl stretching vibration at 2980 cm^{-1}, and the asymmetric and symmetric ester C−O−C stretching vibrations at 1259 and 1159 cm^{-1}, respectively. Because of the low layer thickness of the underlying PGMA (ca. 2 nm thick) the spectrum is dominated by the acrylate film, and typical PGMA bands are overlapped. The Al/PGMA spectrum (Figure 4a—enlarged for better visibility) shows beside the characteristic ester and CH stretching absorptions the epoxide ring mode at 907 cm^{-1} as well as two smaller vibrations in this region indicating residual intact epoxide moieties in the primary polymer layer. These epoxide groups are responsible for the subsequent bonding of the P*t*BA brushes.

After transformation of the P*t*BA layer into a PAA layer the characteristic *t*Bu double band at 1370/1395 cm^{-1} vanished in the IRRA spectrum (Figure 4c). Furthermore, a weakening of the CH_3 band at 2980 cm^{-1} and the ester absorptions were observed. The detected carbonyl band at 1733 cm^{-1} was broadened in the Al/PGMA/PAA spectrum in comparison with the Al/PGMA/P*t*BA spectrum. The slight reduction of the layer thickness measured by ellipsometry (Table 2) is consistent with the mass lost due to splitting off the *t*Bu groups. The calculated grafting densities are in accordance with the layer thicknesses. They decrease slightly after acidolysis of the *t*Bu groups; possibly some chains are removed from the surface by this process. As expected, the advancing water contact angles decrease after splitting off the *t*Bu groups in the polymer brushes both on silicon and aluminum substrates, consistent with the hydrophilic character of the PAA, to 30 and 36°, respectively. These results show that P*t*BA and PAA brushes can be prepared on alumina in the same way as on silica substrates. IRRAS turned out to be the appropriate method to characterize these thin polymer layers on a smooth aluminum substrate and to verify the complete conversion of P*t*BA to PAA using *p*-toluenesulfonic acid as catalyst.

Block Copolymer Single Layers. Three diblock copolymers with different block lengths were used to produce single thin polymer layers on silicon and aluminum substrates in a one-step procedure. These polymers contain a P*t*BA block and a shorter PGMA or P(*t*BA-*co*-PGMA) block as anchor block. The anchor blocks can serve as primer blocks to bond the polymer to the surface. Therefore, the copolymers can be applied to activated Si/SiO_x or Al/AlO_x surfaces directly (without primary polymer layer). After spin-coating, the polymers were linked to the silicon or aluminum surfaces by annealing the wafers at 100 °C for 16 h.[17] The GMA epoxy moieties react with the reactive surface OH groups of the substrate oxides and are able to self-cross-link as shown in Figure 5.

The surface reaction includes an electrophilic attack of an acidic H atom from the surface −OH groups toward the epoxide oxygen inducing either the formation of a Si−O−C bond to the surface or a cross-linking reaction. Both reactions lead to a fixation of the polymer block on the surface. Thus, the GMA anchor block combines the function of a primary polymer layer and a physically adhesive layer. After bonding the layers were stable against the rinsing procedure.

The IRRA spectrum of the block copolymer B2 (P(*t*BA_{250}-*b*-[*t*BA_{57}-*co*-GMA_6])) on aluminum (Figure 6) shows nearly the same absorption bands as the spectrum of the P*t*BA brush prepared in the conventional way via a separate PGMA anchor layer on aluminum (Figure 4). After elimination of the *t*Bu groups by reaction of the layer with *p*-toluenesulfonic acid the double band at 1370/1395 cm^{-1} vanishes entirely indicating a complete reaction. As with the two-layer PGMA/PAA brushes (model brushes) the IRRA spectrum of the block copolymer layer (Figure 6) shows a weakening of the CH_3 band at 2980 cm^{-1} and the other ester absorptions and a broadened carbonyl band at 1733 cm^{-1} in the IRRA spectrum (Figure 6) after splitting off the *t*Bu groups. This proves the conversion to PAA sequences.

After release of the carboxyl moieties the newly generated PAA block is very polar and hydrophilic in nature. The contact angles of the polymer-covered surfaces decrease from θ_a/θ_r =

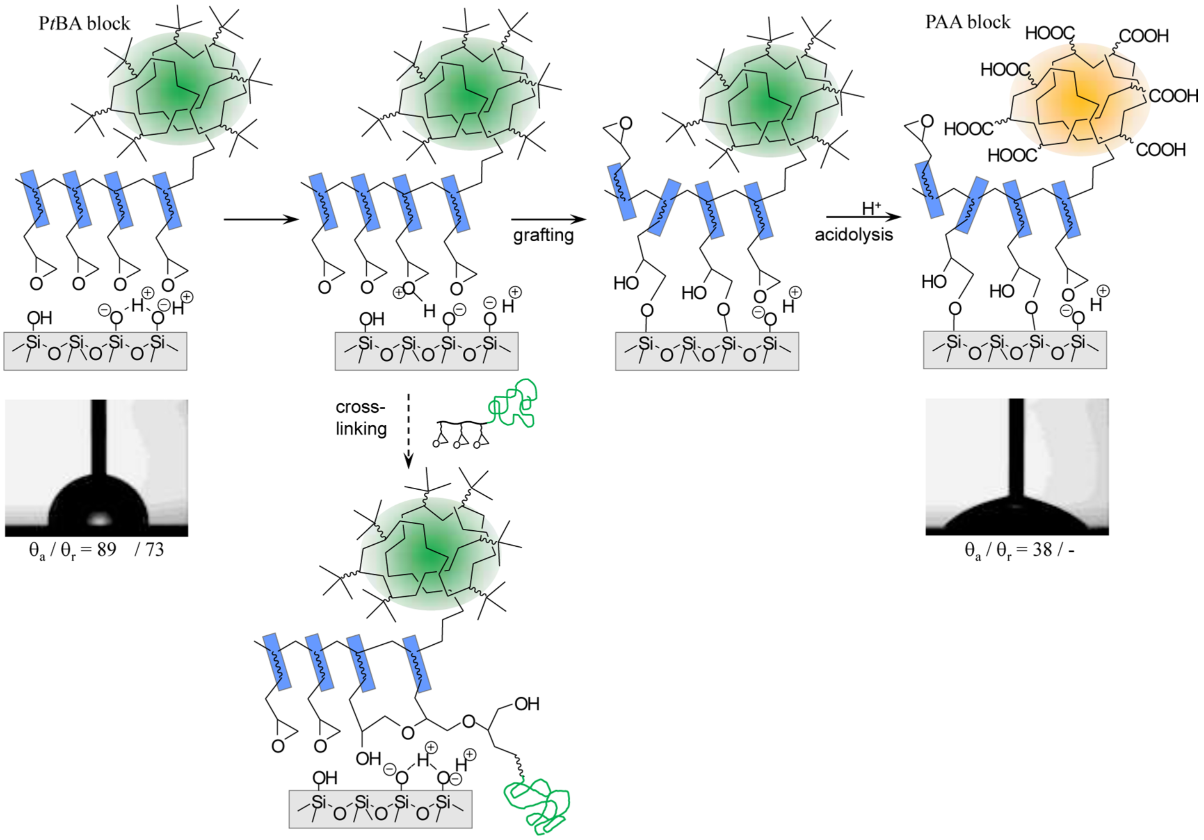

Figure 5. Grafting of the P*t*BA/PGMA diblock copolymers onto a silicon surface, the blue rectangle stands for the methacrylate unit of GMA (>C(CH_3)−COO−).

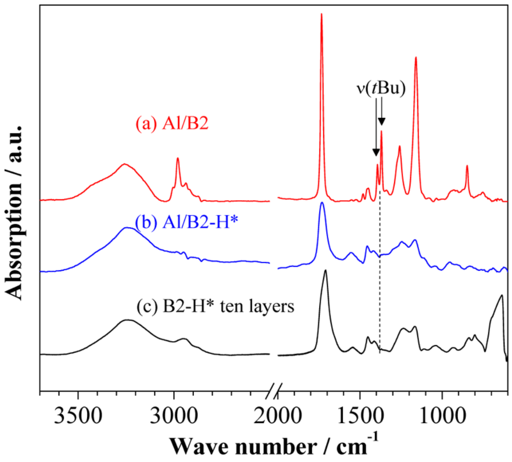

Figure 6. IRRA spectra of (a) block copolymer B2 on aluminum, (b) of block copolymer B2 after acidolysis by *p*-toluenesulfonic acid (on aluminum) and (c) transmission spectrum of ten layers of block copolymer B2 on silicon (annealing and acidolysis by *p*-toluenesulfonic acid after each layer preparation).

89°/73° to θ_a = 38° and a vanishing θ_r. The elimination of the large *t*BA groups causes a layer thickness reduction as with the two-layer PGMA/PAA brushes (see Table 1). In contrast, the grafting density of the three block copolymers seems to be higher after acidolysis due to an increased polymer surface concentration (compare Supporting Information, Table ST1, e.g., $\sigma_{Si/B3}$ = 0.176 chains/nm^2 and $\sigma_{Si/B3-H*}$ = 0.250 chains/nm^2). This may be caused by some water swelling of the hydrophilic PAA layer but shows also that these layers are very stable and show no loss of polymer molecules after this preparation step as detected with the model layers. After additional treatment with boiling water the PAA blocks elongate due to swelling and repulsion of the carboxyl groups. This is confirmed for all investigated diblock copolymers by the increased layer thickness (compare Table 1) and causes an apparently increased grafting density. The single layers on aluminum are somewhat thinner than those on Si wafers indicating a lower grafting density on aluminum. Also the increase of grafting density after acidolysis is less pronounced. This finding corresponds to results of the chemisorption of poly(butadiene epoxide) onto different metal oxide substrates.[7] The reactivity of the substrates correlates well with their isoelectric points (IEP). Thus, a higher reactivity was found for silica surfaces in comparison to alumina.[7] In fact, the IEP of silica and alumina differ considerably, the former amounting to 2−3, whereas the latter amounts to 8−9.[37,38]

The layer thickness and the polymer surface concentration Γ are highest for the block copolymer B3 ($\Gamma_{Si/B3}$ = 11.54 mg/m^2) in comparison to B1 ($\Gamma_{Si/B1}$ = 9.99 mg/m^2) and B2 ($\Gamma_{Si/B2}$ = 9.78 mg/m^2). This is probably due to the longer P*t*BA block in comparison with the other block copolymers.

Figure S2a,b (see Supporting Information) shows exemplary AFM images (topography and phase) of the block copolymer B2 after annealing and extraction and after splitting off the *t*Bu groups. All images show rather smooth, slightly structured surfaces with height variations of ∼1 nm and single, up to 10 nm high, harder asperities that are typical for dry P*t*BA and PAA brushes.[39] The coatings exhibit low roughness parameters with R_q varying from 0.9 to 1.9 nm and R_a varying from 0.6 to 1.2 nm. Similar results were obtained with all three investigated

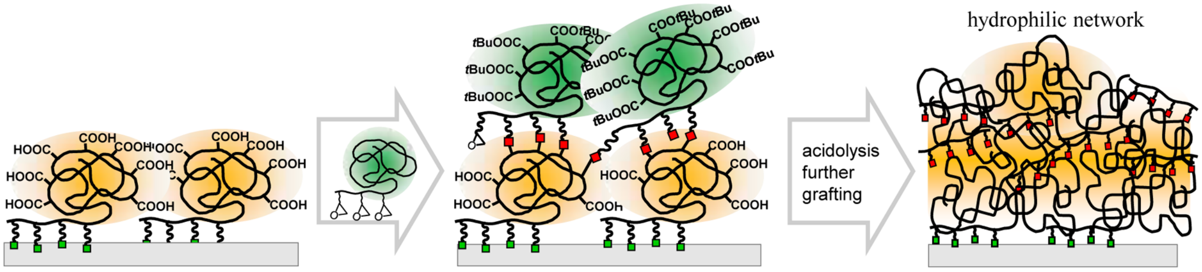

Figure 7. Reactive layer stack approach: Formation of self-cross-linking multilayers; the green squares represent the linkages to the surface hydroxyl groups (Si−O−C), and the red squares stand for ester groups resulting from the reaction of the carboxyl and epoxy groups ($-COO-CH_2-CHOH-$).

block copolymers, except for different film thicknesses (cf. Table 1) as a result of the varying length of the blocks. These differences will be discussed in more detail in the next section.

The "Reactive Layer Stack" Approach. The grafting of P*t*BA/PGMA diblock copolymers (B1, B2, and B3) and the subsequent splitting off of *t*Bu groups was repeated several times to produce copolymer "multilayers" on silicon. With this novel approach it is possible to create sustainable layers with defined thickness and functional groups at the surface. The procedure can be regarded as a special case of the covalent layer-by-layer (LbL) assembly[40] method. For this technique typically two separate polymers with complementary functional groups are used. In our approach we used only one polymer with a dual functionality at which one is only potentially active because it is necessary to remove its protective groups before these functionalities are able to form covalent bonds.

The different composition of the block copolymers was to result in different degrees of cross-linking. The approach benefits on one hand from the potential reactivity of the protected carboxylic acid groups and on the other hand from the versatile reactivity of the epoxy moieties. After spin-coating, the first polymer layer was linked to the surface by annealing as described above. By extraction with THF the ungrafted polymer chains were removed, and only covalently bonded polymer molecules remained in the coating. For the generation of "multilayers" the carboxyl groups in the polymers were released by reaction with *p*-toluenesulfonic acid. Then the next layer was applied and reacted by annealing the wafers at 100 °C for 16 h. In this way the epoxide rings react with the just-released carboxyl groups of the former layer using the intrinsic functionality of these double functional block copolymers (Figure 7). This procedure was continued to obtain up to ten layers.

The thickness of the coatings increased linearly with the number of applied layers as shown in Figure 8. The layers of the three copolymers exhibit different thicknesses in all stages of the multilayer buildup (cf. Table 2, Figure 3). Surprisingly they are not only influenced by the length of the P*t*BA block but also by the length and composition of the shorter PGMA anchor block. The highest layer thicknesses were obtained, as expected, with the copolymer B3 containing the longest P*t*BA block and the highest number of GMA units (~5.3 wt %) in the anchor block. The higher thickness can be due not only to the longer P*t*BA/PAA blocks but also to the higher number of reactive epoxy groups in the copolymer B3 compared to B1 and B2 and the resulting higher number of tethered polymer chains in each step.

Interestingly the layers made of copolymer B1 are thicker than those of copolymer B2 (cf. Table 2, Figure 8), despite its shorter P*t*BA block and the nearly equal number of GMA units in the anchor block. This can be explained by the fact that the PGMA block of copolymer B2 contains additional *t*BA units. Therefore, the reactive groups are less accessible during the reaction. This leads to a lower number of grafted polymers and results consequently in a slightly thinner coating. The surface morphology of the multilayers (Figure S2c, Supporting Information) is similar to that of the single layers of the block copolymer brushes (Figure S2b, Supporting Information) but has a slightly higher overall roughness.

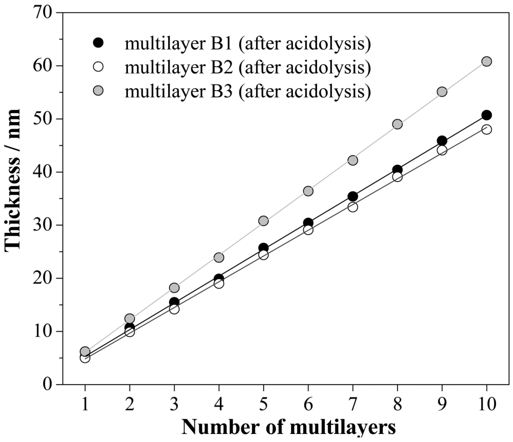

Figure 8. Coating thickness of self-cross-linking multilayers prepared according to the reactive layer stack approach, measured by ellipsometry.

All layers contain a high number of remaining carboxyl groups in the network and are therefore swellable. In situ layer thickness determination of three layers of the polymers B1, B2, and B3 using spectroscopic ellipsometry showed that these layers swell in deionized water to up to 167% (B1), 159% (B2), and 130% (B3) of their dry thickness. This is not as much as examined with the model PAA brushes described in the first part of this study (~350%, 5 nm thick in the dry state). This fact is consistent with the assumed degree of cross-linking in the layers. Actually, the lowest swelling was found for the layer of the polymer with the highest epoxy group content B3. The IR transmission spectra of the ten-layer system of the three block copolymers after splitting off the *t*Bu groups (Figure 6) substantiate the completion of the acidolysis reaction in the layers and show the same bands as in the Al/PGMA/PAA and Al/P(AA-*b*-GMA) and Al/P(AA-*b*-[AA-*co*-GMA]) diblock layers.

Block Terpolymer Single Layers and Their Switching Triggered by Solvents. P(*t*BA-*b*-[*t*BA-*co*-GMA]-*b*-MMA) terpolymers were used to produce single polymer layers on

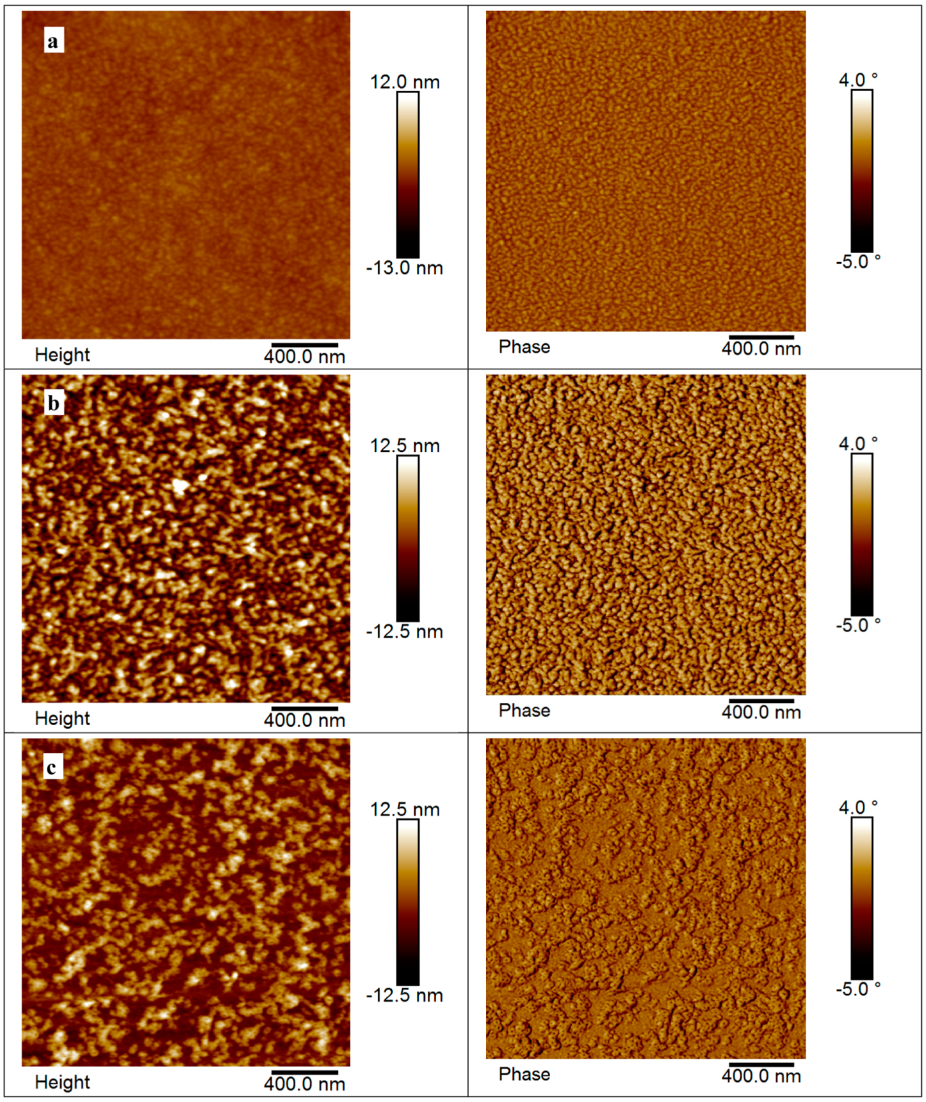

Figure 9. AFM images of layers of (a) the P(tBA$_{194}$-b-[tBA$_{59}$-co-GMA$_{36}$]-b-MMA$_{80}$) terpolymer T1 on silicon wafer, of (b) the same layer after reaction with p-toluenesulfonic acid and treatment with boiling water, (c) after additional treatment with boiling toluene; height images on the left, phase images on the right.

silicon and aluminum substrates. After spin-coating, the polymer layers were linked to the surface by annealing as described above for the diblock copolymers. After the extraction and drying procedure as well as after exposure to different solvents the layers were investigated by AFM (Figures 9 and 11). To allow comparison, all topography images are shown using the same height scale. Phase images were scaled arbitrarily to pronounce typical features of the coatings.

The initially prepared terpolymer film (Figure 9a) exhibits a slightly structured surface with a roughness of $R_q/R_a = 0.6/0.4$. Previous investigations of the properties of the terpolymers had shown that the three different blocks have separate glass transition points if their lengths are not too short.[28] Thus, phase separation may be indicated by a stiffness contrast in the phase images. In this case, bright features in the phase image mark regions that are stiffer than dark areas. The phase images in Figure 9 show, however, also a pronounced influence of the topography. Areas of different brightness can thus be interpreted as manifestation of the separation of phases with different stiffness but also as topography effects.

In a next step the layers were treated with p-toluenesulfonic acid in benzene solution to split off the tBu groups in the terpolymer. As expected the layer thickness of the terpolymer T1 decreased from 12.9 to 9.6 nm. After aqueous treatment of the layer to achieve an orientation of the newly created hydrophilic blocks to the air interface the coating has a coarsely structured surface (Figure 9b), and the roughness increased to $R_q/R_a = 4.4/3.7$. Consequently the phase image is dominated by topography effects. Therefore, the areas of different brightness cannot be clearly interpreted in terms of a possible phase separation. Nonetheless they pronounce details of the surface morphology.

The measured contact angle (62°) points, however, to an incomplete elimination of the tBu groups. After treatment with the hydrophobic solvent toluene the coating adopts a patchy structure with some protrusions (Figure 9c). The elevated structures exhibit small holes—presumably the hydrophilic blocks (the former elevations) have retracted into the now hydrophobic layer. The roughness decreases slightly to $R_q/R_a = 3.2/2.7$, and the contact angle amounts to 91° indicating a switching process (as shown in Figure 12), which implies an orientation of the hydrophobic blocks to the air interface.

Layers of the same terpolymer on aluminum-sputtered silicon wafers were investigated with IRRAS (Figure 10).

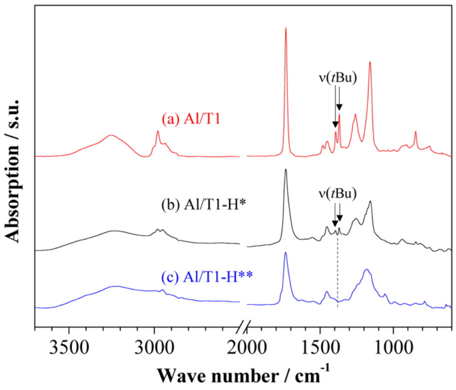

Figure 10. IRRA spectra of layers of the triblock terpolymer T1 on aluminum (a) before acidolysis, (b) after acidolysis with *p*-toluenesulfonic acid (Al/T1−H*), and (c) after acidolysis with methanesulfonic acid (Al/T1−H**).

Figure 10a presents the spectrum of the triblock terpolymer T1 before hydrolysis. After application of the toluenesulfonic acid method (Method A) the spectrum shows only a decrease of the intensity of the double band at 1370/95 cm^{-1} but not its disappearance. This confirms the incomplete splitting off of the *t*Bu groups.

To obtain a complete acidolysis of the P*t*BA blocks in the terpolymer layers, the methanesulfonic acid method (Method B) was applied. This results in a complete vanishing of the double band of the *t*Bu ester visible in the IRRA spectrum of a T1 layer on aluminum. Use of the HCl/dioxane method was ruled out because of the susceptibility of the aluminum layers under these conditions. Layers of T1 on silicon wafers were also treated following method B and investigated with AFM (Figure 11).

The layer thickness measured by ellipsometry is somewhat lower than after applying Method A. For the aqueous treated (hydrophilically switched) layers the AFM images (Figure 11a) show a morphology similar to the "dimple" structure reported for mixed polymer brushes in selective solvents.[41] After hydrophobic toluene treatment the layer appears smoother (Figure 11b). As in Figure 9c small holes are visible that indicate retraction of the former hydrophilic elevations in the hydrophobic layer. As discussed above, the contrast in the phase images can be explained both by phase separation and topography effects.

The roughness of both layers, amounting to R_q/R_a = 3.0/2.5 for the hydrophilic and R_q/R_a = 2.0/1.6 for the hydrophobic layer, is lower than that resulting from Method A. Particularly the differences in the measured contact angles of the coating after the different treatments are evident. Whereas Method A leads to a contact angle of 62°, a contact angle of only 31° is reached for the hydrophilic switched layer obtained with Method B. This corresponds well with the measured data for the PAA brushes and the PAA/PGMA diblock copolymers and is comparable to values from literature.[42] Figure 12 shows schematically the switching process induced by treatment with suitable solvents.

Layers of the terpolymer T2 with a shorter hydrophilic and a longer hydrophobic block were produced by the same method and transformed into amphiphilic polymer layers by Method B. IRRAS measurements on layers of T2 on aluminum surfaces again show clearly the complete elimination of the *t*Bu groups

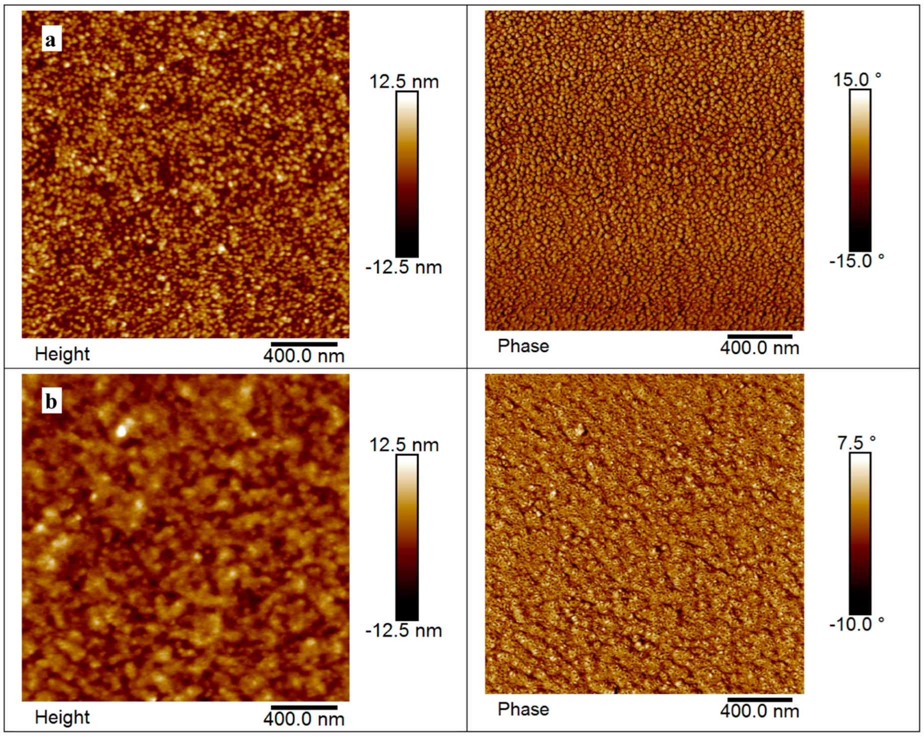

Figure 11. AFM images of layers of (a) terpolymer T1 layer on silicon wafer after treatment with methanesulfonic acid and treatment with boiling water, (b) after additional treatment with boiling toluene; height images on the left, phase images on the right.

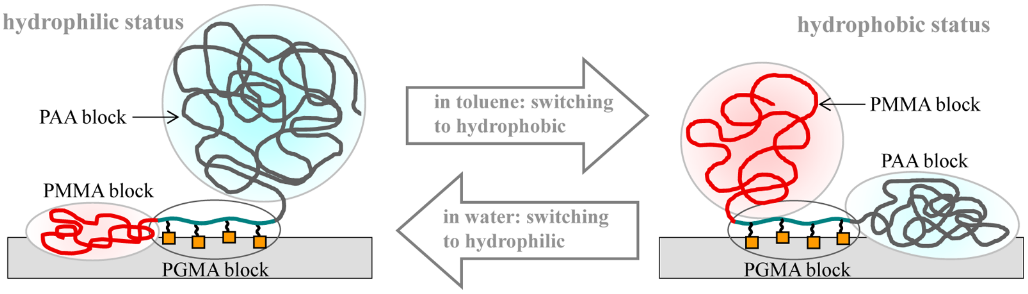

Figure 12. Switching process of the amphiphilic terpolymers induced by solvent treatment after splitting off the *t*Bu groups.

in the layers (Figure S3, Supporting Information). The higher efficiency of methanesulfonic acid as catalyst for cleavage of the *t*Bu ester groups under this conditions results from its stronger acidity. AFM investigations on layers of T2 show a similar dimplelike structure (Figure S4, Supporting Information) as terpolymer T1 after hydrophilic treatment (Figure 11a). The lower distances between the protrusions are very likely due to the lower molar mass of the polymer and particularly the smaller length of the P*t*BA/PAA block. The layer thickness is lower than that of the layers of the terpolymer T1 and decreases even more after splitting off the *t*Bu groups. This may be due to the longer anchoring PGMA block. In case of the aqueous-treated (hydrophilically switched) layers the measured contact angle is 35°, and after hydrophobic treatment it is 84° indicating the switching process of the amphiphilic polymers. Surprisingly the surface morphology is not significantly affected by the switching process. The roughness of the layers (T2 layer: R_q/R_a = 1.0/0.8, T2−H**−H_2O layer: R_q/R_a = 1.9/1.3, T2−H**−toluene layer: R_q/R_a = 1.6/1.1) is somewhat lower than that of the T1 layers likely due to the shorter P*t*BA/PAA block.

In comparison to the common process using a primary polymer layer, that is, the grafting of end-functionalized homopolymers on PGMA films, the described process using copolymers is a simpler procedure. This is important for a transfer to technical coating processes. Furthermore, the use of block co- and terpolymers having an anchor block yields a more stable connection of the polymer layers with the substrates and otherwise enables a bigger variety of the molecular structure, which is important for bottom-up techniques.

CONCLUSIONS

Layers of P*t*BA/PGMA diblock copolymers and P*t*BA/PGMA/PMMA triblock terpolymers were covalently bonded onto oxidic surfaces of silicon and aluminum without additional anchor layer. To obtain hydrophilic layers, P*t*BA was transformed to PAA by splitting off the *t*Bu groups. The acidolysis necessary thereto was examined using IRRAS. In case of the terpolymers a complete transformation reaction was only achieved by using the methanesulfonic acid method. By means of the diblock copolymers a novel reactive layer stack approach was developed, which is based on the ability of these polymers to self-cross-link after splitting off the *t*Bu groups. With this method it was possible to generate covalently cross-linked, functional coatings consisting of very regular mono- or multilayers with a smooth surface and precisely adjustable layer thickness. This method is not limited to the presented P*t*BA/PGMA copolymers but can also be applied to the fabrication of manifold multilayers by using different co- or terpolymers containing protected carboxylic and glycidyl groups. The thickness of the hydrophilic layers presented here was determined both by the length of the P*t*BA block and the composition of the anchor block and increased linearly with the number of layers. The triblock terpolymer layers were amphiphilic after transformation of the P*t*BA block to PAA. Contact angle measurements showed that their wettability can be switched from hydrophilic to hydrophobic by treatment with suitable solvents. AFM investigations showed a dimplelike structure of the hydrophilically switched terpolymers and a change of the morphology after switching to the hydrophobic surface state. The influence of the surface properties (hydrophilicity, hydrophobic−hydrophilic domain structure) of the produced block co- and terpolymer layers on frost formation and ice adhesion is currently being investigated and will be the content of a next paper.

ASSOCIATED CONTENT

Ⓢ Supporting Information

A detailed characterization of the layers of T1, B2, and T2 including further IRRA, ATR spectra, and AFM images. Tabulated grafting parameters of the prepared layers. This material is available free of charge via the Internet at http://pubs.acs.org.

AUTHOR INFORMATION

Corresponding Authors

*Phone: +4937153135859. E-Mail: hoehne@ipfdd.de. (S.H.)
*Phone: +493514658236. E-Mail: uhlmannp@ipfdd.de. (P.U.)

Funding

This work was supported by the Bundesministerium fuer Bildung und Forschung (BMBF) under Project No. 01RI0710AB.

Notes

The authors declare no competing financial interest.

ACKNOWLEDGMENTS

The authors thank G. Adam posthumously who recorded the IRRA spectra and E. Schierz who measured the ATR-FTIR spectra. We thank S. Kehr (Chemnitz University of Technology, Polymer Department, Chemnitz) who carried out the SEC measurements and the BMBF (Project No. 01RI0710AB) for financial support. The authors are thankful to M. Stamm for the initiation of the first anti-icing project, which was a starting point of research with many fascinating aspects, and we appreciate him as very competent counterpart in dialogues and scientific discussions always leading to new ideas and insights.

REFERENCES

(1) Achilleos, D. S.; Vamvakaki, M. End-Grafted Polymer Chains onto Inorganic Nano-Objects. *Materials* **2010**, *3*, 1981−2026.

(2) Zhao, B.; Brittain, W. J. Polymer Brushes: Surface-Immobilized Macromolecules. *Prog. Polym. Sci.* **2000**, *25*, 677−710.

(3) Tsubokawa, N. Modification of Particle Surfaces by Grafting of Functional Polymers. *Spec. Publ.—R. Soc. Chem.* **1999**, *235*, 36−51.

(4) Kickelbick, G.; Schubert, U. Inorganic Clusters in Organic Polymers and the Use of Polyfunctional Inorganic Compounds as Polymerization Initiators. *Monatsh. Chem.* **2001**, *132*, 13−30.

(5) Advincula, R. Polymer Brushes by Anionic and Cationic Surface-Initiated Polymerization (SIP). *Adv. Polym. Sci.* **2006**, *197*, 107−136.

(6) Liu, P. Carbon-Chain Polymers "Grafting From" Inorganic Nanoparticles. *e-Polym.* **2005**, *5*, 732−740.

(7) Köthe, M.; Müller, M.; Simon, F.; Komber, H.; Jacobasch, H. J.; Adler, H. J. Examination of Poly(butadiene epoxide)-Coatings on Inorganic Surfaces. *Colloids Surf., A* **1999**, *154*, 75−85.

(8) Iyer, K. S.; Zdyrko, B.; Malz, H.; Pionteck, J.; Luzinov, I. Polystyrene Layers Grafted to Macromolecular Anchoring Layer. *Macromolecules* **2003**, *36*, 6519−6526.

(9) Motornov, M.; Sheparovych, R.; Lupitskyy, R.; MacWilliams, E.; Hoy, O.; Luzinov, I.; Minko, S. Stimuli-Responsive Colloidal Systems from Mixed Brush-Coated Nanoparticles. *Adv. Funct. Mater.* **2007**, *17*, 2307−2314.

(10) Höhne, S.; Frenzel, R.; Heppe, A.; Simon, F. Hydrophobic Chitosan Microparticles: Heterogeneous Phase Reaction of Chitosan with Hydrophobic Carbonyl Reagents. *Biomacromolecules* **2007**, *8*, 2051−2058.

(11) Quinn, J. F.; Johnston, A. P. R.; Such, G. K.; Zelikin, A. N.; Caruso, F. Next Generation, Sequentially Assembled Ultrathin Films: Beyond Electrostatics. *Chem. Soc. Rev.* **2007**, *36*, 707−718.

(12) Such, G. K.; Quinn, J. F.; Quinn, A.; Tjipto, E.; Caruso, F. Assembly of Ultrathin Polymer Multilayer Films by Click Chemistry. *J. Am. Chem. Soc.* **2006**, *128*, 9318−9319.

(13) Major, J. S.; Blanchard, G. J. Strategies for Covalent Multilayer Growth. 2. Interlayer Linking Chemistry. *Chem. Mater.* **2002**, *14*, 2574−2581.

(14) Park, M. K.; Deng, S. X.; Advincula, R. C. pH-Sensitive Bipolar Ion-Permselective Ultrathin Films. *J. Am. Chem. Soc.* **2004**, *126*, 13723−13731.

(15) Harris, J. J.; DeRose, P. M.; Bruening, M. L. Synthesis of Passivating, Nylon-Like Coatings through Cross-Linking of Ultrathin Polyelectrolyte Films. *J. Am. Chem. Soc.* **1999**, *121*, 1978−1979.

(16) Schuh, K.; Prucker, O.; Rühe, J. Tailor-Made Polymer Multilayers. *Adv. Funct. Mater.* **2013**, *23*, 6019−6023.

(17) Iyer, K. S.; Luzinov, I. Effect of Macromolecular Anchoring Layer Thickness and Molecular Weight on Polymer Grafting. *Macromolecules* **2004**, *37*, 9538−9545.

(18) Zdyrko, B.; Iyer, K. S.; Luzinov, I. Macromolecular Anchoring Layers for Polymer Grafting: Comparative Study. *Polymer* **2006**, *47*, 272−279.

(19) Greene, T. W.; Wuts, P. G. M. *Protective Groups in Organic Synthesis*, 2nd ed; Wiley: New York, 1991.

(20) Husemann, M.; Morrison, M.; Benoit, D.; Frommer, K. J.; Mate, C. M.; Hinsberg, W. D.; Hedrick, J. L.; Hawker, C. J. Manipulation of Surface Properties by Patterning of Covalently Bound Polymer Brushes. *J. Am. Chem. Soc.* **2000**, *122*, 1844−1845.

(21) Douvas, A.; Argitis, P.; Misiakos, K.; Dimotikali, D.; Petrou, P. S.; Kakabakos, S. E. Biocompatible Photolithographic Process for the Patterning of Biomolecules. *Biosens. Bioelectron.* **2002**, *17*, 269−278.

(22) Davis, K. A.; Matyjaszewski, K. Atom Transfer Radical Polymerization of tert-Butyl Acrylate and Preparation of Block Copolymers. *Macromolecules* **2000**, *33*, 4039−4047.

(23) Wu, T.; Gong, P.; Szleifer, I.; Vlcek, P.; Subr, V.; Genzer, J. Behavior of Surface-Anchored Poly(acrylic acid) Brushes with Grafting Density Gradients on Solid Substrates: 1. Experiment. *Macromolecules* **2007**, *40*, 8756−8764.

(24) Ionov, L.; Houbenov, N.; Sidorenko, A.; Stamm, M.; Luzinov, I.; Minko, S. Inverse and Reversible Switching Gradient Surfaces from Mixed Polyelectrolyte Brushes. *Langmuir* **2004**, *20*, 9916−9919.

(25) Synytska, A.; Stamm, M.; Diez, S.; Ionov, L. Simple and Fast Method for the Fabrication of Switchable Bicomponent Micropatterned Polymer Surfaces. *Langmuir* **2007**, *23*, 5205−5209.

(26) Steiner, G.; Sablinskas, V.; Savchuk, O.; Bariseviciute, R.; Jähne, E.; Adler, H. J.; Salzer, R. Characterization of Self Assembly Layers of Octadecanephosphonic Acid by Polarisation Modulation FT-IRRA Spectroscopy Mapping. *J. Mol. Struct.* **2003**, *661*, 429−435.

(27) Kita-Tokarczyk, K.; Junginger, M.; Belegrinou, S.; Taubert, A. Amphiphilic Polymers at Interfaces. *Adv. Polym. Sci.* **2011**, *242*, 151−201.

(28) Kreider, A.; Weber, B.; Stenzel, V.; Tornow, C.; Grunwald, I. Natural Frost Protection Coupling Antifreeze Proteins to a PU Coating Inhibits Ice Deposition. *Eur. Coat. J.* **2011**, No. 5, 34−39.

(29) Esser-Kahn, A. P.; Trang, V.; Francis, M. B. Incorporation of Antifreeze Proteins into Polymer Coatings Using Site-Selective Bioconjugation. *J. Am. Chem. Soc.* **2010**, *132*, 13264−13269.

(30) Lv, J. Y.; Song, Y. L.; Jiang, L.; Wang, J. J. Bio-Inspired Strategies for Anti-Icing. *ACS Nano* **2014**, *8*, 3152−3169.

(31) Kretschmer, K.; Uhlmann, P.; Stamm, M.; Frenzel, R.; Simon, F. Permanent Coating of Surfaces for Inhibiting and/or Preventing them from Icing Up, and Use Fort that Purpose. U.S. Patent No. 8,202,620 B2, 2012.

(32) Höhne, S.; Uhlmann, P. The Synthesis of Functional Blockco- and Terpolymers Containing Polyglycidyl Methacrylate Blocks. *J. Polym. Sci., Part A: Polym. Chem.*, Accepted.

(33) Werner, C.; Eichhorn, K. J.; Grundke, K.; Simon, F.; Grahlert, W.; Jacobasch, H. J. Insights on Structural Variations of Protein Adsorption Layers on Hydrophobic Fluorohydrocarbon Polymers Gained by Spectroscopic Ellipsometry (Part I). *Colloids Surf., A* **1999**, *156*, 3−17.

(34) Rauch, S.; Eichhorn, K. J.; Oertel, U.; Stamm, M.; Kuckling, D.; Uhlmann, P. Temperature Responsive Polymer Brushes with Clicked Rhodamine B: Synthesis, Characterization and Swelling Dynamics Studied by Spectroscopic Ellipsometry. *Soft Matter* **2012**, *8*, 10260−10270.

(35) Magonov, S. N.; Elings, V.; Whangbo, M. H. Phase Imaging and Stiffness in Tapping-Mode Atomic Force Microscopy. *Surf. Sci.* **1997**, *375*, L385−L391.

(36) *Atlas der Polymer- und Kunststoffanalyse*, 2nd ed; Carl Hanser Verlag: München-Wien, VCH Verlagsgesellschaft: Weinheim-Basel-Cambridge-New York, 1988; Vol. 2 (I), bI.

(37) Lewis, J. A. Colloidal Processing of Ceramics. *J. Am. Ceram. Soc.* **2000**, *83*, 2341−2359.

(38) Jara, A. A.; Goldberg, S.; Mora, M. L. Studies of the Surface Charge of Amorphous Aluminosilicates Using Surface Complexation Models. *J. Colloid Interface Sci.* **2005**, *292*, 160−170.

(39) Gupta, S.; Uhlmann, P.; Agrawal, M.; Lesnyak, V.; Gaponik, N.; Simon, F.; Stamm, M.; Eychmüller, A. Covalent Immobilization of Quantum Dots on Macroscopic Surfaces Using Poly(acrylic acid) Brushes. *J. Mater. Chem.* **2008**, *18*, 214−220.

(40) Bergbreiter, D. E.; Liao, K.-S. Covalent Layer-by-Layer Assembly—an Effective, Forgiving Way to Construct Functional Robust Ultrathin Films and Nanocomposites. *Soft Matter* **2009**, *5*, 23−38.

(41) Minko, S.; Müller, M.; Usov, D.; Scholl, A.; Froeck, C.; Stamm, M. Lateral versus Perpendicular Segregation in Mixed Polymer Brushes. *Phys. Rev. Lett.* **2002**, *88*, 35502.

(42) Uhlmann, P.; Ionov, L.; Houbenov, N.; Nitschke, M.; Grundke, K.; Motornov, M.; Minko, S.; Stamm, M. Surface Functionalization by Smart Coatings: Stimuli-Responsive Binary Polymer Brushes. *Prog. Org. Coat.* **2006**, *55*, 168−174.